ELSEVIER

Advances in Water Resources 25 (2002) 1335–1348

Advances in Water Resources

www.elsevier.com/locate/advwatres

Ecohydrology of water-controlled ecosystems

A. Porporato [a,*], P. D'Odorico [b], F. Laio [a], L. Ridolfi [a], I. Rodriguez-Iturbe [c]

[a] *Dipartimento di Idraulica, Trasporti ed Infrastrutture Civili, Politecnico di Torino, Corso Duca degli Abruzzi, 24, 10129 Torino, Italy*
[b] *Department of Environmental Sciences, University of Virginia, Charlottesville, VA 22904-4123, USA*
[c] *Department of Civil and Environmental Engineering and Center for Energy and Environmental Studies, Princeton University, Princeton, NJ 08544, USA*

Received 14 November 2001; received in revised form 11 March 2002; accepted 11 March 2002

Abstract

Ecosystem dynamics in arid and semiarid climates are strongly dependent on the soil water availability which, in turn, is the result of a number of complex and mutually interacting hydrologic processes. This motivates the development of a process-based framework for the analysis of the soil water content in the root zone at the daily time scale. This paper reviews the results that the authors have obtained using a probabilistic–mechanistic model of soil water balance for the characterization of the seasonal regimes of soil moisture with different combinations of climate, soil, and vegetation. Average seasonal soil water content and level-crossing statistics have been used to study conditions of water stress in vegetation. The same framework has been applied to the analysis of the impact of interannual climate fluctuations on the seasonal regime of soil moisture and water stress.

1. Introduction

The spatial and temporal dynamics of soil moisture has been often investigated in connection to its interactions with a number of hydrologic, atmospheric, and ecologic processes. In fact, the soil water content controls the rates of rainfall infiltration, deep percolation, and runoff generation; soil moisture conditions affect the heat budget of both soil and near-surface atmosphere, leading to an important coupling between processes taking place at the soil surface and in the planetary boundary layer. Soil moisture controls also the dynamics of terrestrial ecosystems, especially in conditions of scarce water availablity. In such environments, the rates of transpiration, carbon assimilation, and biomass production are often limited by the soil water content during the growing season. In these conditions of water-limited transpiration, vegetation undergoes a state of water stress, which depends (in terms of duration and frequency) on the plant physiology and the local pedological and climatic characteristics. The nutrient cycle and the budget of organic matter in the soil are also strongly affected by the dynamics of soil moisture.

This paper reviews some of the analytic probabilistic tools we have recently developed to address the study of the temporal dynamics of soil moisture at a point and its implications on plant ecosystems. Due to the random character of precipitation, a stochastic approach has been used to investigate the soil water balance, and a probabilistic characterization of soil moisture dynamics has been obtained in terms of probability distribution, moments [9,26,29], and crossing statistics [20,22] of soil water content. The analysis of the stochastic soil water balance has privileged a process-based approach instead of a mere fitting of some stochastic models to the data. This has allowed the development of mechanistic models of ecosystem dynamics in water-limited environments (e.g., [27,28]). In particular, these models have shown how different climate, soil, and vegetation characteristics can affect the regime of soil moisture during the growing season in plant ecosystems [10]. They also provide a quantitative criterion to assess to which extent the nonlinearities and feedbacks embedded in the dynamics of soil moisture are able to enhance the effect of climate fluctuations on the seasonal regime of soil moisture [5,23].

The present analysis is limited to cases where the soil moisture dynamics may be considered in statistically steady conditions during the growing season. For an assessment of the importance of transient conditions at

* Corresponding author.
E-mail address: porporato@polito.it (A. Porporato).

0309-1708/02/$ - see front matter
PII: S0309-1708(02)00058-1

the beginning of the growing season the reader is referred to Laio et al. [11] and Rodriguez-Iturbe et al. [30].

2. Probabilistic modeling of soil moisture dynamics and water balance

This section presents a brief summary of the analytical tools characterizing the probabilistic soil moisture dynamics as studied in detail by Rodriguez-Iturbe et al. [26] and Laio et al. [9]. The probabilistic representation of the soil water balance is expressed by the stochastic differential equation

$$nZ_r \frac{\mathrm{d}s}{\mathrm{d}t} = I(s,t) - E(s) - L(s), \tag{1}$$

where n is the porosity, Z_r is the active depth of soil, s is the relative soil moisture content, $I(s,t)$ is the rate of infiltration from rainfall, $E(s)$ is the rate of evapotranspiration, and $L(s)$ is the rate of leakage or deep infiltration.

Rainfall is stochastically represented as a Poisson process of storm arrivals in time with rate λ, each storm having a depth h, modeled as an exponentially distributed random variable with mean α. Rainfall results in an infiltration depth into the soil, $I(s,t)$, which is taken to be the minimum of h and $nZ_r(1-s)$ to reflect the fact that only a fraction of h can infiltrate when the rainfall amount exceeds the storage capacity of the soil column. Excess rainfall produces runoff according to the mechanism of saturation from below. Canopy interception, which is responsible for the capture and subsequent direct evaporation of some of the precipitation prior to its arrival at the soil surface, is included in the model by assuming a threshold of rainfall depth, Δ, below which no water effectively penetrates the canopy. Then, analytically, the only change necessary is to modify the rate of storm arrivals, λ, to $\lambda' = \lambda e^{-\alpha\Delta}$ [26]. All model results are interpreted at the daily time scale.

The term $E(s)$ incorporates losses due to evaporation from the soil and transpiration from the plant. At the daily time scale $E(s)$ may span three regimes: it linearly increases with s from 0 at the hygroscopic point, s_h to E_w, at the wilting point, s_w (soil evaporation regime). For larger values of s $E(s)$ has a linear rise (stressed evapotranspiration regime) from E_w at s_w to E_{max} at s^*, where s^* is the soil moisture level at which the plant begins to close stomata in response to water stress and E_{max} is the climate and vegetation dependent maximum daily evapotranspiration rate. For values of s exceeding s^* evapotranspiration is decoupled from soil moisture and remains constant at E_{max} (unstressed evapotranspiration regime), which represents the average daily evapotranspiration rate during the growing season under well-watered conditions.

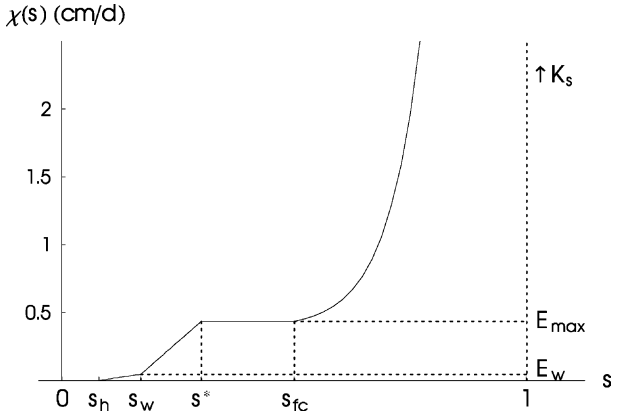

Fig. 1. Soil water losses (evapotranspiration and leakage), $\chi(s)$, as function of relative soil moisture for typical climate, soil, and vegetation characteristics in semiarid ecosystems. After Laio et al. [9].

Assuming no interaction with the underlying soil layers and water table and the absence of significant topographic gradients, $L(s)$ represents vertical percolation with unit gradient

$$L(s) = \frac{K_s}{e^{\beta(1-s_{fc})} - 1}\left[e^{\beta(s-s_{fc})} - 1\right], \tag{2}$$

where K_s is the saturated hydraulic conductivity, s_{fc} is the field capacity, and $\beta = 2b + 4$ with b the pore size distribution index. The leakage losses predicted by Eq. (2) have very similar behavior to those given by the commonly adopted power law representation (e.g., [3]), yet for reasons of analytical tractability Eq. (2) is adopted over the customary power law. The sum of the evapotranspiration and leakage losses $\chi(s) = E(s) + L(s)$ is shown in Fig. 1; its behavior is very similar to the ones both employed in similar studies (e.g., Cordoba and Bras [38]) and found in field investigations (e.g., Salvucci, 2001). The values of s_h, s_w, s^* and s_{fc} are related to the corresponding soil matric potentials Ψ_{s_h}, Ψ_{s_w}, Ψ_{s^*}, and $\Psi_{s_{fc}}$ through the empirically determined soil–water retention curves (e.g., [3]).

The analytical expression for the steady state probability density function (pdf) of soil moisture as well as the expressions for the water balance components during the growing season are given in Laio et al. [9] under the assumption of statistically homogeneous growing season climate.

Fig. 2 shows an analysis of the role of changes in the frequency of storm events λ on the soil moisture pdf, while the mean rainfall depth α and the climatic control on E_{max} are kept constant. A coarser soil texture corresponds to a consistent shift of the pdf toward drier conditions. The shape of the pdf also undergoes marked changes and resembles the one empirically found (e.g., Salvucci [39]). The broadest pdfs are found for shallower soils.

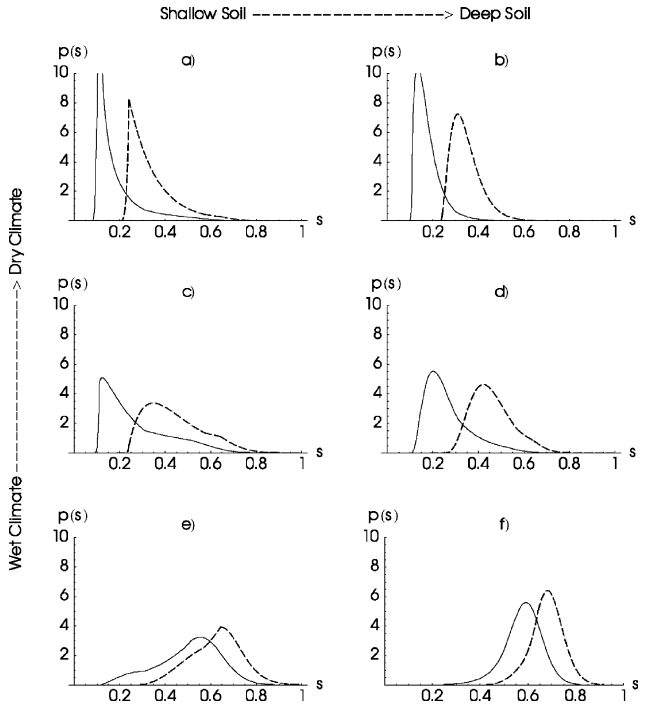

Fig. 2. Examples of pdfs of soil moisture for different type of soil, soil depth, and mean rainfall rate. Continuous lines refer to loamy sand ($K_s = 100$, $n = 0.42$, $s_h = 0.08$, $s_w = 0.11$, $s^* = 0.31$, $s_{fc} = 0.52$), dashed lines to loam ($K_s = 20$, $n = 0.45$, $s_h = 0.19$, $s_w = 0.24$, $s^* = 0.57$, $s_{fc} = 0.65$). Left panels correspond to $Z_r = 30$ cm, right panel to 90 cm. Top, center, and bottom graphs have a mean rainfall rate λ of 0.1, 0.2, and 0.5 d^{-1} respectively. Common parameters to all graphs are $\alpha = 1.5$ cm, $\Delta = 0$ cm, $E_w = 0.01$ cm/d, and $E_{max} = 0.45$ cm/d (after Laio et al. [9]).

An indication of the impacts on vegetation of the probabilistic dynamics of soil moisture is provided by the analysis of particular realizations of soil moisture traces. Fig. 3 shows a superposition of two traces of soil moisture with the same rainfall realization for the case

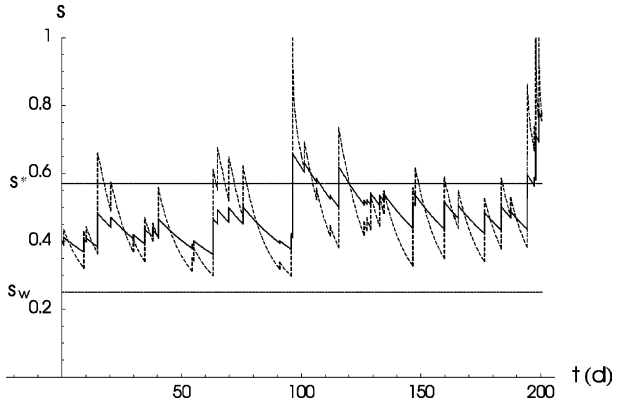

Fig. 3. Example of traces of soil moisture for the same rainfall sequence in a loamy soil with different depths ($\alpha = 1.5$ cm, $\lambda = 0.2$ d^{-1}, $\Delta = 0$ cm, $E_w = 0.01$ cm/d, $E_{max} = 0.45$ cm/d). Continuous line refers to $Z_r = 90$ cm, dashed line to $Z_r = 30$ cm. The other parameters are the same as in Fig. 2c and d (- - -) (after Laio et al. [9]).

of a loam with two different depths of active soil. In both cases the levels of soil moisture s^* and s_w are the same. The mean soil moisture is also approximately the same in both cases. The continuous line, corresponding to the deeper soil, is almost always between s^* and s_w, differently from the shallower soil where the trace lively jumps and decays between low and high soil moisture levels. The following section discusses how this different behavior in the soil moisture dynamics is important to plants of different types, and which are the possible responses of vegetation and the different strategies of adaptation to water stress.

2.1. Long-term water balance

The different terms of the long-term water balance are the averages of the respective components of the soil moisture dynamics. Rainfall is first partitioned into interception, runoff, and infiltration. Infiltration is then divided into leakage and evapotranspiration. For purposes of describing vegetation conditions, the amount of water transpired can be further divided into water transpired under stressed conditions and water transpired under non-stressed conditions. The water balance is thus

$$\langle R \rangle = \langle I \rangle - \langle Q \rangle - \langle E_s \rangle - \langle E_{ns} \rangle - \langle L \rangle, \tag{3}$$

where $\langle R \rangle$ is the mean rate of the rainfall, $\langle I \rangle$ is canopy interception, $\langle Q \rangle$ represents the mean rate of runoff, $\langle E_s \rangle$ and $\langle E_{ns} \rangle$ are the mean rates of evapotranspiration under stressed and non-stressed conditions, respectively, and $\langle L \rangle$ is leakage.

Fig. 4 presents examples of the dependence of the water-balance components—normalized by the mean rainfall rate—on some characteristics of rainfall regime, soil, and vegetation. The influence of the rainfall rate λ is shown in Fig. 4a for the case of a shallow loam. Since interception is a linear function of the rainfall rate, it is not surprising that the fraction of water intercepted remains constant once it is normalized by the total rainfall, $\alpha\lambda$. The percentage of runoff increases almost linearly. More interesting is the interplay between leakage and the two components of evapotranspiration. The fraction of water transpired under stressed conditions rapidly decreases, while the evapotranspiration under non-stressed conditions evolves in a much more gradual manner. As discussed by Porporato et al. [20], this last aspect has interesting implications for vegetation productivity. It is clear that in semiarid conditions most of the water that actually reaches the soil is lost by evapotranspiration (in particular transpiration), a result in agreement with many field observations (e.g., [6,32, 33,35]).

Fig. 4b shows the role of the active soil depth in the water balance. For relatively shallow soils there is a strongly non-linear dependence on soil depth of all the

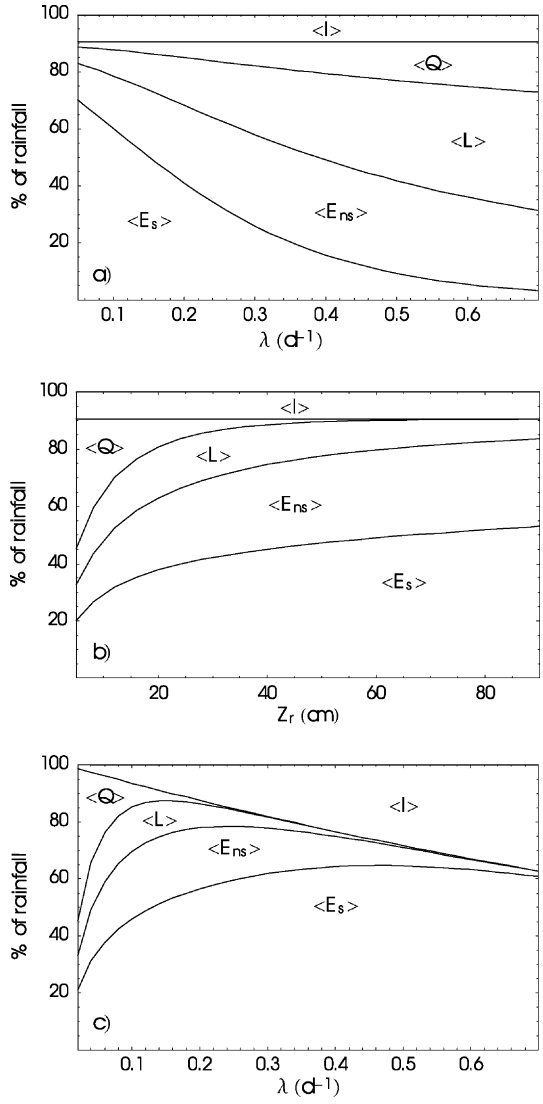

Fig. 4. Components of the water balance normalized by the total rainfall. (a) Water balance as a function of the mean rainfall rate λ, for a shallow loamy soil ($Z_r = 30$ cm, $\alpha = 2$ cm). (b) Water balance as a function of the soil depth Z_r, for a loamy sand ($\alpha = 2$ cm, $\lambda = 0.2$ d^{-1}). (c) Water balance for a loamy sand as a function of the ratio between rainfall rate of occurrence (λ) and mean rainfall depth (α) for a constant mean total rainfall during a growing season, $\Theta = 60$ cm. Other common parameters are $E_w = 0.01$ cm/d, $E_{max} = 0.45$ cm/d, and $\Delta = 0.2$ cm (after Laio et al. [9]).

components of the water balance (with the obvious exception of interception, which is constant because the rainfall is constant). For example, changing from $nZ_r = 5$ to 20 the amount of water transpired is practically doubled.

Fig. 4c shows the terms of the water balance when both the frequency, λ, and the average storm depth, α, change but the total amount of rainfall in a growing season (i.e. $\alpha\lambda$) is kept constant. The result is interesting, due to the existence of two opposite mechanisms regulating the water balance. On the one hand, for a given seasonal amount of rain, runoff production strongly depends on the ratio between soil depth and the mean depth of rainfall events. The rapid decrease of runoff is thus somewhat analogous to that in the first part of Fig. 4b, where a similar behavior was produced by an increase in soil depth. On the other hand interception increases almost linearly with λ. The interplay between these two mechanisms determines a maximum of both leakage and evapotranspiration at moderate values of λ (of course the position of the maxima changes according to the parameters used). This is particularly important to vegetation, since the mean transpiration rate is directly linked to productivity of ecosystems (e.g., [14, p. 383]). The role not only of the amount, but also of the frequency of rainfall in soil moisture dynamics, especially in water-controlled ecosystems (see also [18]), is made clear by the existence of an optimum for transpiration (a surrogate for productivity). The particular position of this maximum in the parameter space is governed by the interplay of all the mechanisms acting in the soil–water balance, namely the intensity and amount of rainfall, interception, the active soil depth, and the non-linear losses due to evapotranspiration and leakage.

The steady state analysis of Eq. (2) is most appropriate for the study of water-controlled ecosystems where rainfall is mostly concentrated in a warm growing season, and winter is usually temperate and dry. As a consequence, in those cases the starting soil moisture condition at the beginning of the growing season is not very different from the rest of the season and transients due to seasonality are generally not significant. Different ecosystems which are examples of these conditions are the savannas of South Africa [35], the shrublands in southern Texas, at least for most of the growing season [1,34], and the shortgrass steppe in Colorado [32]. In contrast, transient soil moisture dynamics and climatic seasonality can be important in other semiarid environments, especially at the beginning of the growing season. As discussed by Rodriguez-Iturbe et al. [30] and Laio et al. [11], this is related to the climatic conditions (e.g., seasonality), to the soil depth, and to the ratio between losses and rainfall input during the months preceeding the growing season. Typical cases include Mediterranean climates (e.g., [15–17]) and the Patagonian steppe [8,19]. Temperate forests in the northwest United States (e.g., [37]) are also heavily controlled by transient soil moisture conditions. In these cases, rainfall and temperature are markedly out of phase, and the dormant season becomes a period of consistent soil–water storage to be used during the following growing season.

3. Plant water stress

This section briefly reviews the analytical tools characterizing the plant conditions in water-limited ecosystems as presented in [20].

A concept of static vegetation water stress, ζ, has been developed to relate the actual value of soil moisture to two levels of the same variable associated with important changes in the physiological activities of the plant, namely the point at which transpiration (and thus photosynthetic activity) starts being reduced, s^*, and the point at which plants begin to wilt, s_w. These two levels correspond to the point of incipient and complete stomatal closure, respectively. Static stress is assumed to be equal to 0 when soil moisture is above s^* and equal to 1 when soil moisture is at or below s_w. In between these soil moisture levels, the static stress is given by

$$\zeta(t) = \left[\frac{s^* - s(t)}{s^* - s_w}\right]^q, \tag{4}$$

where q is a measure of the non-linearity of the effects of soil moisture deficit on plant conditions.

The simple relationship between ζ and s permits the derivation of the pdf of ζ as a derived distribution of the steady state pdf of soil moisture [20]. The mean of the pdf of ζ includes the periods when ζ is 0 and is therefore not very representative of actual vegetative conditions. The mean value of water stress given that the plant is under stress, $\bar{\zeta}'$, is more meaningful for our purposes and is calculated by only considering the part of the pdf corresponding to ζ values greater than 0, i.e.

$$\bar{\zeta}' = \frac{\bar{\zeta}}{P(s^*)}, \tag{5}$$

where $P(s^*)$ is the probability of a given plant to be under stress and $\bar{\zeta}$ is the mean of the pdf of the static water stress ζ.

Besides the information given by $\bar{\zeta}'$, the dynamical aspects of the water deficit process, namely the duration and frequency of the stress periods, should also be taken into account to fully describe the plant stress conditions. To this purpose, Porporato et al. [20] derived the expressions for the mean length, $\bar{T}_\xi$, of an excursion below an arbitrary soil moisture threshold, ξ, as well as the mean number, $\bar{n}_\xi$, of such intervals during the growing season. The two crucial thresholds to which these expressions have been explicitly applied are again s_w and s^*.

The above information on the stress intensity, its mean duration, and its frequency of occurrence may be combined to define the dynamical water stress, $\bar{\theta}$. This is an overall indicator of the condition of the plant under given edaphic and climatic factors:

$$\bar{\theta} = \begin{cases} \left(\dfrac{\bar{\zeta}'\bar{T}_{s^*}}{kT_{\text{seas}}}\right)^{\frac{1}{\sqrt{\bar{n}_{s^*}}}} & \text{if } \bar{\zeta}'\bar{T}_{s^*} < kT_{\text{seas}}, \\ 1 & \text{otherwise}, \end{cases} \tag{6}$$

where k is an indicator of plant resistance to water stress and T_{seas} is the duration of the growing season. The reader is referred to Porporato et al. [20] for the derivation and full discussion of the dynamical water stress function, $\bar{\theta}$.

4. Optimal plant conditions

It was shown in Fig. 4 that, given a total rainfall during the growing season, there is an intermediate value of the storm frequency λ that produces a maximum of evapotranspiration and possibly optimal conditions for plant growth. Along the same lines, Fig. 5 shows that, for a constant seasonal rainfall, the interplay between λ and α produces a minimum of dynamic water stress, again for intermediate values of λ. Such evidences provide a richer connotation to the concept of effective rainfall (i.e. an event which is intense enough to stimulate biological processes, particularly growth and reproduction), whose importance is well known in the ecology of arid and semiarid ecosystems (e.g., [18]). The number of such effective events during the growing season is strongly linked to the interplay between λ and α in controlling the total rainfall. Moreover, the concept of vegetation-effective rainfall (and thus also the definition of optimal environmental conditions for vegetation) is not just related to climatic conditions, but is intimately coupled with soil and plant properties, such as rooting depth, soil texture, and physiological plant characteristics. The same rainfall event, in fact, can be effective for shallow-rooted plants and completely ineffective for deep-rooted ones. An interesting field evidence of the importance of Z_r is given by Sala and Lauenroth [31], who found that an event of 0.5 cm, that is often considered not very important for some deep-rooted vegetation (e.g., [4]), is fundamental for *Bouteloua gracilis*, a short C_4 grass of the Colorado steppe which has most of its roots in the first centimeters of the soil.

An example of the connection between rainfall regime and rooting depth is shown by Fig. 5a, where the vegetation dynamic water stress is calculated for different values of Z_r and λ, keeping fixed the total rainfall during the growing season at $\Theta = 50$ cm. The dynamic stress is equal to 1 in a large region near the upper right corner of the diagram, where the values of α are low and the soil depth is high. In fact, with a low α the percentage of vegetation-effective rainfall decreases because interception becomes more important. In such conditions plants that are unable to develop a shallow rooting system end up with suffering permanent damages, because in deeper soils the level of s is consistently too low to sustain effective transpiration. The dynamic stress $\bar{\theta}$ is high also for very low values of λ, mainly because in this case the rainfall events become too rare and plant survival becomes very difficult. For the specific plant parameters and the particular total rainfall considered in this example, the area of best fitness (minimum dynamic stress) covers a wide range of values of λ but tends to be limited

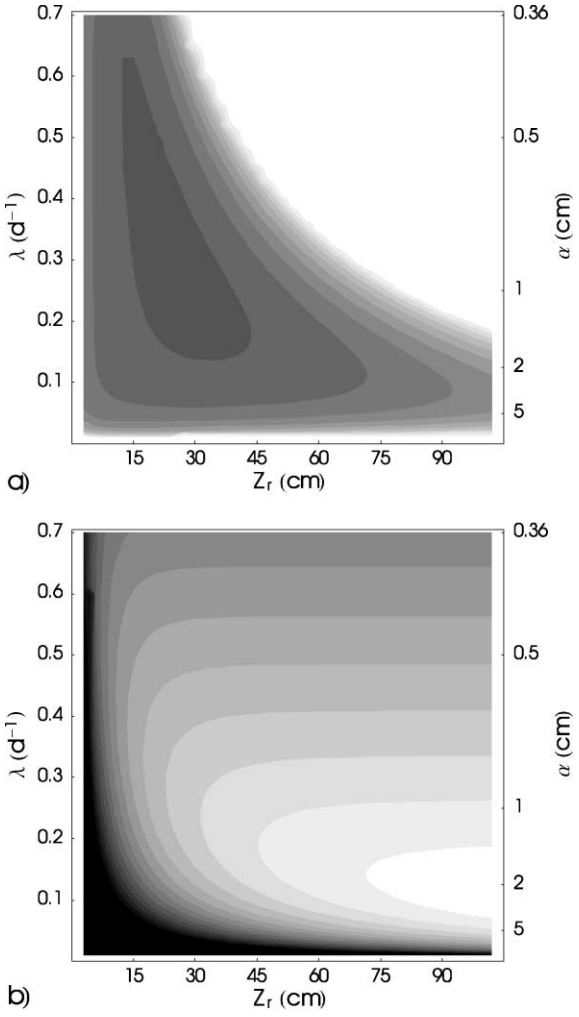

Fig. 5. Optimal vegetation conditions in terms of plant water stress and total evapotranspiration. (a) Mean dynamic water stress and (b) total evapotranspiration during the growing season versus timing and amount of rainfall and active soil depth, keeping fixed the total amount of rainfall per growing season. In (a), $\bar{\theta} = 1$ in the white part of the diagram, $\bar{\theta} < 0.5$ in the darker area of the diagram, and the fixed interval between two adjacent contour lines is 0.05; in (b), evapotranspiration is more than 92% of incoming rainfall in the white part of the diagram, less then 50% in the black area, with a distance of 3% between adjacent contour lines. T_{seas} is 200 d, $q = 2$, and $k = 0.5$. Canopy interception is included here with a value of $\Delta = 0.1$ cm (after Porporato et al. [20]).

to medium–low rooting depths (dark gray area in Fig. 5a). Of course, the region of optimal condition for a given amount of rainfall may be different when the transpiration characteristics of the plants or the soil properties are changed. Therefore, even when dealing with only a single plant resource (e.g., soil moisture), multiple optimal conditions for vegetation may be a possible way for the coexistence of very diverse species and the maximization of species diversity. The investigation of such aspects could help clarify how hydrological processes drive and control many aspects of the biological richness of ecosystems.

A minimum of the plant water stress, however, does not alone suffices to define the optimal conditions for a given type of vegetation. A more comprehensive measure of favorableness of an environment, besides the plant water stress, should also take into account a measure of the effective plant productivity and reproduction capacity. A preliminary indication of this can be obtained by confronting the optimum fitness region of Fig. 5a with analogous regions of maximum evapotranspiration, which frequently can be assumed to be a good surrogate for the productivity of a plant (e.g., [2,14,18]). Fig. 5b shows total evapotranspiration as a function of Z_r and λ, keeping the total amount of rainfall fixed to $\Theta = 50$ cm. The unfavorable conditions for vegetation are now found near the left bottom corner of the diagram, where evaporation is low because of an excessive production of runoff and leakage due either to a high amount of rainfall per event or to a low rooting depth. Very high values of λ are also unfavorable, because with very light rainfall events canopy interception becomes increasingly more important. The maximum evapotranspiration is attained in this case for deep soils with values of α of about 2 cm (white area in Fig. 5b).

In water-controlled ecosystems, optimal plant conditions are likely to be subordinated to the achievement of a compromise between low water stress and high productivity, which is better accomplished through some specific combinations of climate, soil, and vegetation parameters. For the particular example of Fig. 5, in the case of very frequent but light rainfall events (say, $\lambda > 0.3$) the controlling factor is the plant water stress. Thus shallow rooted species are preferred both because of a better exploitation of the incoming water (the amount of water transpired is approximately the same except for very low values of Z_r) and because of less severe conditions of water deficit. In case of more intense and infrequent rainfall events (e.g., $\lambda \leqslant 0.3$) the preferable range of Z_r shifts toward deeper values where one finds both high transpiration (e.g., productivity) and low plant water stress.

The dynamic water stress has been used by Porporato et al. [21] to investigate optimal plant conditions and the coexistence of trees and grasses in the Kalahari precipitation gradient. As shown in Fig. 6, differences in water balance and plant water stress between trees and grasses generate varying preferences for vegetation types along the transect, with deeper-rooted trees favored in the more mesic regions of the northern Kalahari and grasses favored in the drier zones of the southern Kalahari. The point of equal stress, which could be interpreted as identifying a region of tree–grass coexistence, is found at around $\lambda = 0.2\ \mathrm{d}^{-1}$, which corresponds to a total rainfall of approximately 420 mm for the seven-month period of the wet season (October to April). The fact that the slope of the two curves near the crossing point is fairly mild may contribute to explain the existence of a wide

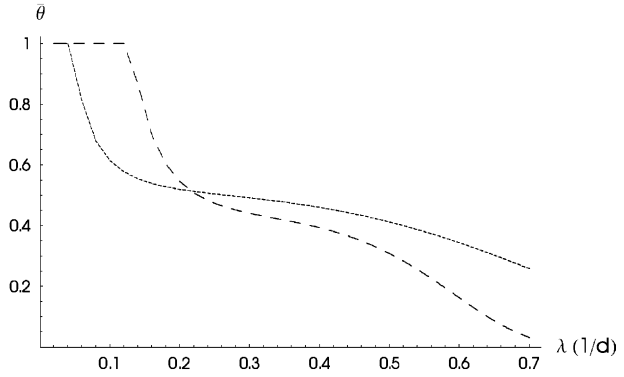

Fig. 6. Behavior of the dynamical water stress as a function of the mean rainfall rate for trees (- - -) and grasses (· · ·) along the Kalahari precipitation gradient ($\alpha = 1$ cm, $T_{seas} = 210$ d) (after Porporato et al. [21]).

region suitable for tree–grass coexistence at average rainfall rates. The pronounced interannual variability of both rainfall parameters might further enhance the possibility of coexistence by randomly driving the ecosystem from an increase in grasses during dry years to tree encroachment during wet years. A similar mechanism has been found to be a possible reason for tree–grass coexistence in the savannas of southern Texas, where a strong interannual rainfall variability induces marked fluctuations in the percentage of tree canopy coverage (see [1,10,27]).

The analysis of optimal plant conditions in cases where the initial soil moisture content is important needs a suitable modification of the dynamic water stress given before. Such an extension was carried out by Rodriguez-Iturbe et al. [30]. In particular, they investigated how intensive or extensive use of water (i.e. plants that rely on a dependable winter recharge, as opposed to others that quickly respond to the intermittent and uncertain rainfall during the growing season) affects soil moisture dynamics and thus also plant water stress. We refer the reader to that paper for a discussion of climate, soil, and vegetation characteristics leading to the dominance or possible coexistence of these two strategies of water use.

5. The role of soil texture in the Colorado shortgrass steppe: the inverse texture effect

Soil texture has been shown to influence patterns of vegetation structure in water-controlled ecosystems through its impact on soil water availability (e.g., [18]). This is specially important in an area where water availability is the key variable driving the structure and function of the ecosystem. Noy-Meir [18] introduced the concept of "inverse soil texture effect" as a diagnostic of arid and semiarid ecosystems. According to his interpretation of this effect, climate and soil texture interact to give rise to different patterns of soil water availability with the result that the same plant can exist with lower seasonal amount of rainfall on coarse soils.

The well documented shortgrass steppe in north-central Colorado, with its large variability in soil texture, was used by Laio et al. [10] as a case study to investigate the role of soil texture on the soil water dynamics and on the water stress of its dominant species, *B. gracilis*. Other studies in this region have focused on the influence of soil texture on the probability of recruitment of *B. gracilis* [13] or on soil water storage patterns within different soil texture sites [36]. The occurrence of the inverse soil texture effect may be a possible explanation for the dominance over time of *B. gracilis* at this site.

The mean dynamic water stress, $\bar{\theta}$, combines the information contained in the soil moisture crossing properties and the static water stress to provide a quantitative index of the overall condition of a plant under given edaphic and climatic factors. Fig. 7a and b show USDA soil texture triangles illustrating the $\bar{\theta}$ values for *B. gracilis* during the relatively dry and relatively wet years, respectively.

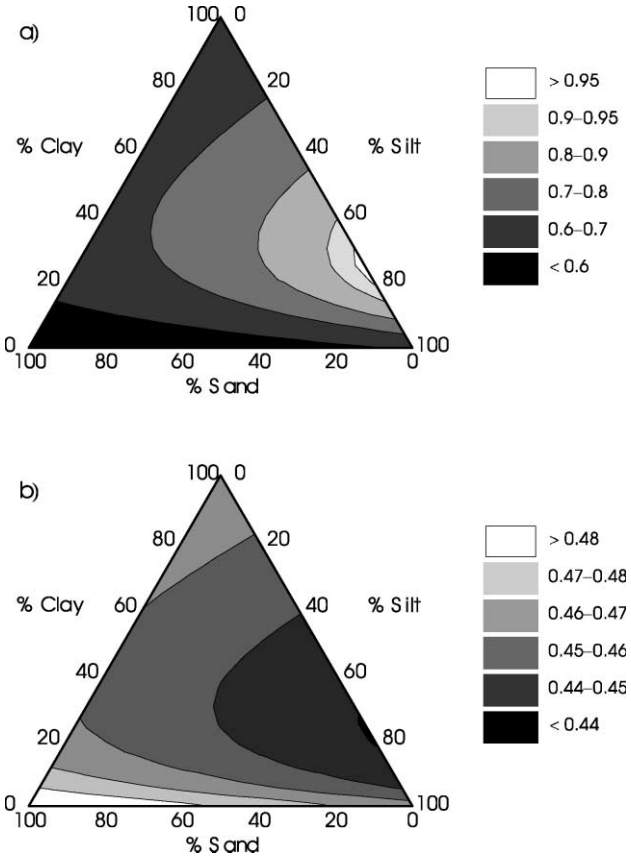

Fig. 7. Dynamic water stress on the soil texture triangle for *B. gracilis*: (a) under a relatively dry climate, $\alpha = 0.576$ cm and $\lambda = 0.17$ d^{-1}; and (b) under a relatively wet climate, $\alpha = 0.674$ cm and $\lambda = 0.28$ d^{-1}. $T_{seas} = 183$ d, $q = 3$, and $k = 0.5$ (after Laio et al. [10]).

Fig. 7a shows the $\bar{\theta}$ values to be in the 0.575 (sand; black in the figure) to 0.95 (silty clay/silt loam; white in the figure) range, indicating large sensitivity to soil texture in the overall condition of *B. gracilis* under a relatively dry climate. Under such a climate, this C_4 grass performs better in a coarse soil than in a fine soil. In contrast, Fig. 7b shows $\bar{\theta}$ to be in the 0.44 (silty clay/silty loam; black in the figure) to 0.48 (sand; white in the figure) range, indicating reduced sensitivity to soil texture in the overall condition of *B. gracilis* under a relatively wet climate. In addition, for these wetter conditions this C_4 grass performs better in a fine soil than in a coarser one.

For the relatively dry and intermediate climates the region of minimum sufferance is therefore the "sand region" while for the relatively wet climate, the most favorable soil texture region is the "silty loam region". This result from the dynamic model of soil moisture supports the "inverse texture effect" described by Noy-Meir [18, p. 37]): "The same vegetation can occur at lower rainfall on coarse soils than it does on fine ones. The balance point between the advantage of coarser texture and its disadvantage occurs somewhere between 300 and 500 mm rainfall". In order to investigate this further, Laio et al. [10] computed the mean dynamic stress for *B. gracilis* on three soil types, namely sand, clay, and silty loam, for a continuously varying total growing season rainfall Θ (Fig. 8). The values of α and λ were linearly increased from those corresponding to the relatively dry case ($\Theta = 179$ mm) to those of the relatively wet year ($\Theta = 345$ mm). Fig. 8 shows how the preferential soil type for this grass differs as a function of Θ. For a relatively dry year *B. gracilis* is more fit in sand than in silty loam or clay (Fig. 7a). Its better fitness in coarse soils than in fine ones is true for Θ up to approximately 260 mm. As the total growing season rainfall increases above that value, it undergoes less mean dynamic stress in fine soils than in coarse soils. Taking into account that the total growing season (April–September) rainfall is approximately 70% of the total annual rainfall for this area [12], the point at which coarse soils become better than fine soils for *B. gracilis*, or viceversa, occurs at an annual rainfall of approximately 370 mm, which is in the range of values indicated by Noy-Meir [18]. *B. gracilis* can do well on coarse soils on years or sites where annual total rainfall is low and it can also do well on fine soils on years or sites where annual rainfall is higher.

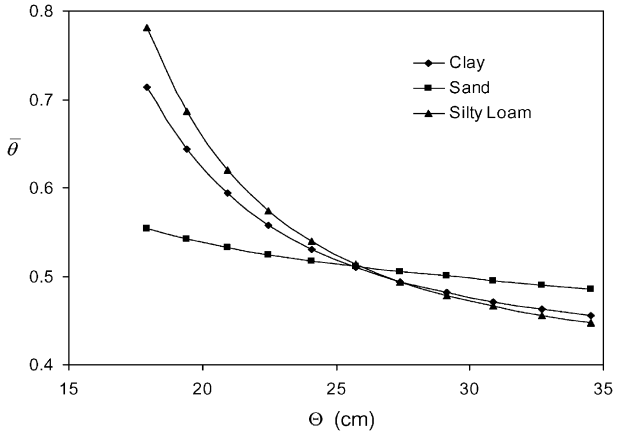

Fig. 8. Dynamic water stress $\bar{\theta}$ for *B. gracilis* at CPER as a function of the total incoming rainfall during the growing season, Θ. The parameters α and λ vary linearly with Θ. $T_{seas} = 183$ d, $k = 0.5$ and $q = 3$ (after Laio et al. [10]).

Further analyses of the role of soil texture on the soil moisture dynamics and plant conditions have been carried out by Fernandez-Illescas et al. [7] who considered a wider range of climatic and vegetative scenarios as well as all the textural classes within the USDA soil textural triangle. Moreover, they investigated the ability of soil texture to encourage grass/tree coexistence at the savanna site of La Copita, Texas, under interannual fluctuations in the rainfall conditions.

6. The impact of interannual rainfall fluctuations

The variability of precipitation during a growing season is reflected in the high-frequency fluctuations of soil moisture observed, for example, in Fig. 3. In many arid and semiarid regions there is also a strong interannual variability in the regime of precipitation (i.e. in the frequency and in the depth of storms) and, as a consequence, in the soil moisture dynamics as well (e.g., [24]). This year-to-year variability is in part controlled by general circulation and global climate patterns which enhance the fluctuations in the growing-season rainfall regime compared to the typical variability of a Poisson process with constant coefficient.

Through the action of the long-term water balance, both such types of fluctuations may be at the origin of temporal niches of soil moisture availability for plants, which in turn may affect the coexistence of species and the development of different strategies of soil water use. The interannual variability, in particular, may explain the long-term evolution of some plant ecosystems.

D'Odorico et al. [5] and Ridolfi et al. [23] showed how changes in the rainfall regime lead to year-to-year fluctuations in the average seasonal soil moisture which may have bimodal distribution. D'Odorico et al. [5] analyzed the characteristics of the rainfall regime during the growing season of the last 60 or 70 years in southwest Texas, where the impact on vegetation of the pronounced interannual rainfall fluctuations have been well documented (e.g., [1,27,28]).

Following the stochastic characterization of rainfall as a marked Poisson process, the interanual variability of the rainfall regime was characterized through the

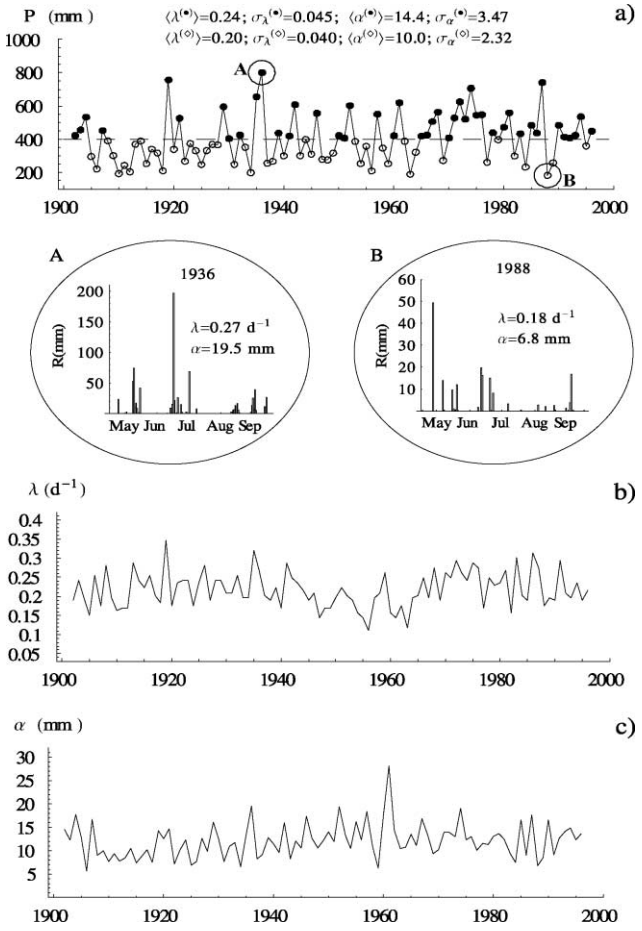

Fig. 9. Analysis of the rainfall regime during the growing season at Luling (Texas) based on daily data of precipitation: (a) time series of total seasonal rain (May 1st–September 30th). (b) Time series of the estimated rate of arrival of storms, λ. (c) Time series of the average storm depth, α (after D'Odorico et al. [5]).

sequence of values of average storm depth, α, and frequency of storm arrivals, λ, estimated for each growing season using the available records of daily precipitation.

The values of the parameters λ and α characterizing the rainfall regime during the growing season were evaluated for a set of locations, along with their mean and variance. Fig. 9 shows a typical example of time series of seasonal precipitation and of average seasonal values of storm depth, α, and frequency, λ.

The histograms of frequency distribution of these parameters (Fig. 10) are always unimodal and the coefficients of variation of λ and α are similar in value, though in Texas the relative variability of λ was found to be somewhat weaker than that of α. In all cases, two-parameter gamma distributions provided a good fit to the histograms.

A correlation analysis of λ and α has shown that both the autocorrelations and the cross correlations are very weak for α and λ. Thus, these parameters may been modeled as independent gamma-distributed random variables.

6.1. Probabilistic behavior of average soil moisture

The mean value of soil moisture during a growing season, $\langle s \rangle$, was used by D'Odorico et al. [5] to characterize the impact of climate on water balance and vegetation in arid and semiarid regions. A Monte Carlo procedure was implemented to numerically estimate the probability distribution of $\langle s \rangle$ resulting from the random interannual fluctuations of λ and α. Pairs of values, $\{\lambda, \alpha\}$, were repeatedly sampled from their gamma distributions and the corresponding values of $\langle s \rangle$ were estimated using their analytical expression obtained through the solution of s [26].

Fig. 11 shows an example of the distributions of $\langle s \rangle$ for given climate, soil, and vegetation, with different hypotheses on the coefficients of variation of α and λ. For high values of the coefficient of variation of any or both of these parameters, one observes the emergence of a bimodal behavior driven by the variability of the climatic

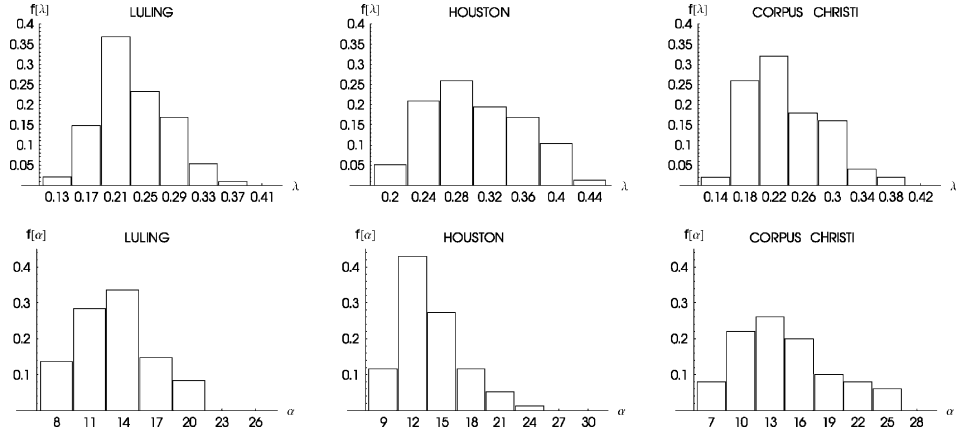

Fig. 10. Frequency distribution of the rate of arrival of storms, λ, and of average storm depth, α, estimated from daily data of precipitation for some locations in Texas during the growing season (after D'Odorico et al. [5]).

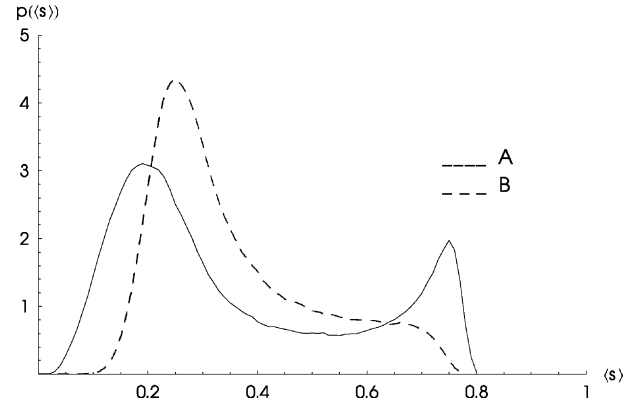

Fig. 11. Pdf of the average soil moisture during the growing season. The parameters for soil and vegetation are as follows: $n = 0.431$; $Z_r = 1.40$ m; $K_s = 9.5 \times 10^{-6}$ m/s; $s_1 = 0.8$; $s^* = 0.36$; $E_{max} = 3.2$ mm/day. The rainfall is characterized by $\langle\alpha\rangle = 12.4$ mm/storm and $\langle\lambda\rangle = 0.21$ storms/day, with coefficients of variation: (A) CV$[\alpha] = 0.45$; CV$[\lambda] = 0.23$. (B) CV$[\alpha] = 0.22$; CV$[\lambda] = 0.11$ (after D'Odorico et al. [5]).

parameters. This behavior suggests that the system tends to switch between two preferential states, one characterized by high average soil moisture and the other by low average soil moisture conditions. This feature has important implications for the dynamics of plant ecosystems because it implies that these systems are subject to soil moisture conditions which are far from the long-term average. The bimodal behavior disappears when the fluctuations become weaker, clearly showing the importance of the intensity of the fluctuations.

In systems forced by fluctuations of the same intensity, different combinations of climate, soil, and vegetation lead to different statistical distributions of $\langle s\rangle$. As an example, the role of climate can be investigated by estimating the pdf of $\langle s\rangle$ for different mean values of α and λ while keeping unchanged their coefficients of variation as well as all the other parameters representative of soil and vegetation. Fig. 12a shows that the larger the mean seasonal rainfall, the higher the peak in the mode corresponding to the wet regime. In a similar way, drier climates lead to an increasingly higher dry mode until the other mode disappears. For the climate of Texas (solid line of Fig. 12a), we observe the emergence of two preferential states with the mode corresponding to the dry regime being more pronounced than the one of the wet regime.

The probabilistic structure of $\langle s\rangle$ is also very sensitive to the soil and vegetation characteristics. Fig. 12b shows the probability distribution of $\langle s\rangle$ computed for different values of E_{max}. We observe that, as expected, lower rates of evapotranspiration enhance the wet mode, while higher values of E_{max} correspond to larger values in the dry mode until the wet mode finally disappears. The roles of the active soil depth is shown in Fig. 12c remarking how the double-mode behavior disappears for shallow soils. The probability distributions of $\langle s\rangle$ have been determined also with different soil (Fig. 12d). The occurrence of a second mode on the wet regime seems to be favored in fine-grain soils because of their ability to retain the water longer, while the dry mode is much more pronounced in coarser grain soils.

The bimodal character of the probability distribution of the average soil moisture under fluctuating climatic conditions is due to the non-linearity embedded in the dynamics and in particular to the non-linear dependence of the rates of evapotranspiration and percolation on

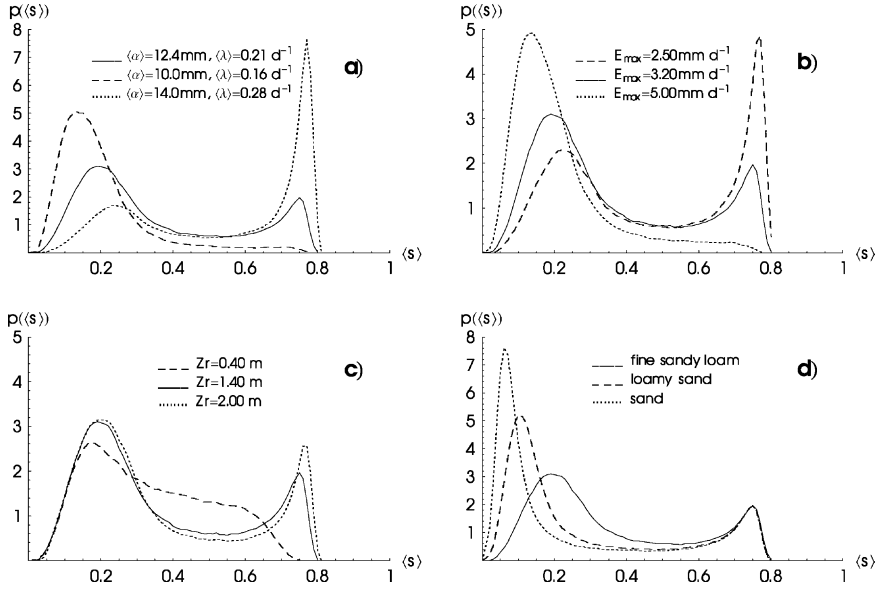

Fig. 12. Probability density function of the average soil moisture during the growing season. The parameters for soil and vegetation are the same as in Fig. 11, apart from (a) where CV$[\alpha] = 0.45$; CV$[\lambda] = 0.23$ (after D'Odorico et al. [5]).

relative soil moisture, as well as to the dependence of rainfall infiltration on the available soil water storage capacity.

The possible occurrence of double modes in the probability distribution of soil moisture had been previously reported by Rodriguez-Iturbe et al. [25] through another stochastic model of soil water balance in a completely different framework. Their results showed how preferential states may arise in the soil moisture dynamics at the continental scale as a consequence of the coupling between soil surface and atmosphere. The present analysis focuses on a much smaller scale where there is no recycling of moisture between the land and the atmosphere. Since here the mean soil moisture during the growing season is statically linked to the rainfall parameters for that same period, the rate of switching of $\langle s \rangle$ between the two possible states is determined only by the interannual rainfall fluctuations.

The effect of interannual rainfall fluctuations on the mean crossing properties of soil moisture has been studied by Ridolfi et al. [23] completing the analysis of the impact of interannual rainfall variability on the seasonal dynamics of soil moisture.

7. Tree–grass coexistence and optimization of water stress

Rodriguez-Iturbe et al. [27,28] proposed a model to analyze the coexistence of trees and grasses in savannas based on the optimization of plant water stress. A simple definition of water stress was used which is based on a similar expression to that of Eq. (4) where the soil moisture conditions are given by the average values typical of a growing season, i.e.

$$\xi = \begin{cases} \left[\dfrac{s^* - \langle s \rangle}{s^* - s_w}\right]^q & \text{for } s < s^*, \\ 0 & \text{otherwise.} \end{cases} \tag{7}$$

The value of q represents the non-linear response of vegetation to water deficit. Admittedly this representation of water stress is much simpler than the one provided by the dynamic water stress, nevertheless it embeds most of the effect of soil moisture dynamics on vegetation. The model considers a region heterogeneous in soil and vegetation represented by a grid with square cells which correspond to the average canopy coverage (e.g., 5 m × 5 m or 10 m × 10 m). The area covered by roots of the individual plants is larger than the individual cell to allow for competition among neighboring vegetation. The whole region is assumed to be under the same climatic conditions.

From the definition of seasonal water stress (7), one can visualize that different kinds of vegetation will undergo different stress conditions under any prescribed climatic characteristics. An example of this is shown in Fig. 13 for a typical case of trees and grasses. The different values of E_{max}, s^* and s_w for trees and grasses lead to stress–soil water curves that intersect regardless of the particular exponent, q, used in equation (7). When a site is considered in isolation from its neighbors and no spatial interactions take place, soil moisture values above A favor trees while soil moisture values below A favor the existence of grasses.

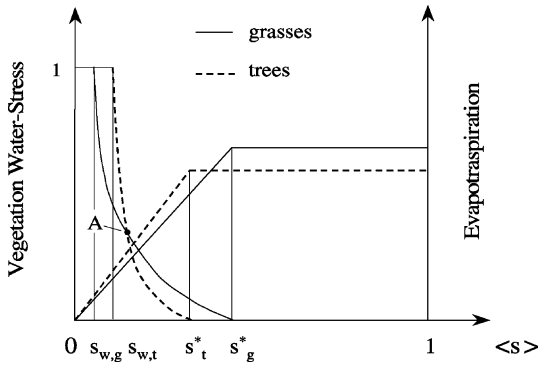

Fig. 13. Diagram used to model plant responses to water stress for mean typical parameter values of trees and grasses (after Rodriguez-Iturbe et al. [28]).

Competition for soil moisture is assumed to take place locally and depend on the levels of stress of neighboring plants. The spatial dynamics controlling the competition for soil moisture is assumed to globally minimize the vegetation stress resulting from deficits of soil water content. No attempt is made to model the temporal dynamics of the vegetation system: given the soil, climate and vegetation fields we allow for local (spatial) competition for water (each cell with its eight nearest neighbors) and we estimate the corresponding field of soil moisture. Of all the possible scenarios of competition and configurations of the field of soil moisture, that leading to a minimum global vegetation stress (i.e. mean seasonal stress throughout the simulation domain) was assumed the one that takes place. In this scheme, the competition for soil moisture is always local but the goal is a global optimum. The analysis was repeated with different (assigned) compositions of the vegetation fields. The best fitness to the environmental conditions (i.e. climate and soils) was assumed to be associated with compositions of vegetation corresponding to the minimum global stress.

The spatial scheme of interaction presented above was applied to the case of Nylsvley savanna [27,28,35]. In this case the vegetation layer was composed by *Burkea africana* (woody) and *Eragostris pallens* (herbaceous). As shown in Fig. 14, the minimum-stress situation corresponds to a tree canopy density near 35% which matches quite well the values of 30–40% observed in the field [35]. With no spatial interactions, the optimal condition is a field 100% covered with grass, while the spatial dynamics lead to mixtures of trees and grasses that reduce global vegetation stress. Fig. 14 also shows the dependence of

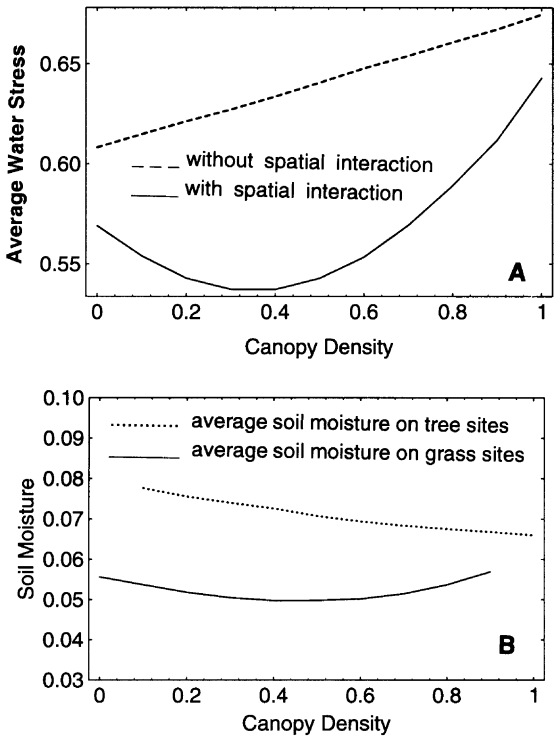

Fig. 14. (a) Average water stress and (b) average soil moisture in tree and grass sites as a function of tree canopy cover for broad-leaf savannas at Nylsvley (after Rodriguez-Iturbe et al. [28]).

average soil moisture at the tree and grass sites as a function of tree canopy density. As expected, tree sites show a higher average soil water content than grass sites with values that agree well with those observed in the region (as inferred from Fig. 6.6 in [35]).

The impact of climatic fluctuations was studied by repeating the experiments under different rainfall conditions. A 20% wetter climate leads to a global minimum vegetation stress with 100% trees. Similarly a 20% drier climate yields a minimum-stress state at 100% grass. It was also observed that the spatial interactions which lead to a more efficient use of soil moisture also yield higher evapotranspiration rates.

The optimization of water stress was also employed to investigate the effect of climatic fluctuations on tree–grass coexistence in the savannas of southern Texas [28] where significant changes in the canopy density have been observed to be associated with interannual rainfall variability [1].

The climatic conditions responsible for the canopy densities observed in 1941, 1960 and 1983 were assumed to be those in the preceding decades. The mean growing-season precipitation (from May through September) was 395 mm in 1931–1941, 339 mm in 1950–1960 and 412 mm in 1973–1983.

The minimization of global vegetation stress as function of woody plant density resulted in the stress values shown in Fig. 15. One observes in Fig. 15 that for

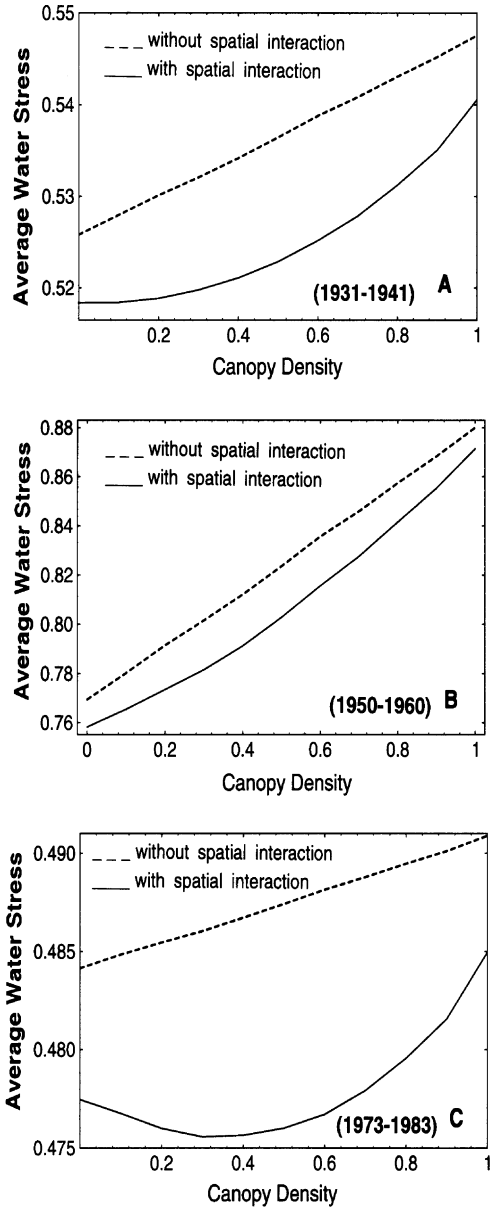

Fig. 15. Average water stress of Eq. (7) with $q = 2$ as a function of tree canopy coverage for vegetation at La Copita. Rainfall conditions refer to months from May through September in Alice during (a) 1931–1941 (average rainfall 395 mm), (b) 1950–1960 (average rainfall 339 mm) and (c) 1973–1983 (average rainfall 412 mm) (after Rodriguez-Iturbe et al. [28]).

1941, 1960 and 1983 the minimum vegetation stress occurs when the density of woody plants is about 15%, 0% and 35%, respectively. These values agree quite well with the observed ones for those dates (13%, 8% and 36%, respectively).

8. Conclusions

The study of soil moisture dynamics is instrumental to the understanding of a number of ecological pro-

cesses, especially in water-limited ecosystems. This paper has reviewed some probabilistic models developed for a process-based analysis of the temporal dynamics of soil water content at a point. The probabilistic characterization of the soil moisture regime has been expressed through its probability distribution, mean, and level-crossing statistics and these have been used in the analysis of the duration and frequency of water stress in vegetation, leading to the formulation of the concepts of static and dynamic water stress.

This framework has been applied in the study of the spatial dynamics of soil moisture and water stress in savannas, suggesting a possible explanation for the observed coexistence of herbaceous and wood vegetation in these ecosystems. The effect of climatic fluctuations on the soil moisture dynamics has been finally investigated through the analysis of how average seasonal values of water content and stress duration are affected by the interannual variability of the precipitation regime. The non-linearity of the underlying dynamics may lead to the emergence of a double mode in the probability distribution of seasonal soil moisture, suggesting the existence of two preferential states in the interannual variability of average soil water content, and the enhancement of the impact of climate fluctuations on vegetation in arid and semiarid ecosystems.

Ongoing research is applying this probabilistic framework to the study of the soil nitrogen and carbon cycles: a process-based model of nutrient dynamics is being developed which estimates the mass balance of carbon and nitrogen in the different pools of soil organic and inorganic matter accounting for the dependence of the processes of mineralization, nitrification, denitrification, root uptake, and leaching on the soil water content. This approach leads to an analysis of the effect of the random forcing of precipitation on the seasonal dynamics of nutrients, and suggests a new criterion for the mechanistic modeling of soil nitrogen availability, nutrient uptake, biomass production, and plant growth in water-limited ecosystems. Further research is investigating the role of topography in the spatial variability of soil moisture, nutrients, and vegetation; the annual variability of soil water content due to the seasonality of precipitation and evapotranspiation; and the probabilistic modeling of biogenic emission of trace gases from terrestrial ecosystems.

References

[1] Archer S, Scifres C, Bassham CR, Maggio R. Autogenic succession in a subtropical savanna: conversion of grassland to thorn woodland. Ecol Monogr 1988;58:90–102.

[2] Boyer JS. Plant productivity and environment. Science 1982;218:443–8.

[3] Clapp RB, Hornberger GN. Empirical equations for some soil hydraulic properties. Water Resour Res 1978;14(8):601–4.

[4] Coupland RT. Ecology of mixed prairie in Canada. Ecol Monogr 1950;20:271–315.

[5] D'Odorico P, Ridolfi L, Porporato A, Rodriguez-Iturbe I. Preferential states of seasonal soil moisture: the impact of climate fluctuations. Water Resour Res 2000;36(8):2209–19.

[6] Eagleson PS, Segarra RI. Water-limited equilibrium of savanna vegetation systems. Water Resour Res 1985;21:1483–93.

[7] Fernandez-Illescas C, Porporato A, Laio F, Rodriguez-Iturbe I. The role of soil texture in water limited ecosystems. Water Resour Res 2001;37(12):2863–72.

[8] Golluscio RA, Sala OE, Lauenroth WK. Differential use of large summer rainfall events by shrubs and grasses: a manipulative experiment in the Patagonian steppe. Oecologia 1998;115(1–2):17–25.

[9] Laio F, Porporato A, Ridolfi L, Rodriguez-Iturbe I. Plants in water-controlled ecosystems: active role in hydrologic processes and response to water stress—II. Probabilistic soil moisture dynamics. Adv Water Resour 2001;24(7):707–23.

[10] Laio F, Porporato A, Fernandez-Illescas CP, Rodriguez-Iturbe I. Plants in water-controlled ecosystems: active role in hydrologic processes and response to water stress—IV. Discussion of real cases. Adv Water Resour 2001;24(7):745–62.

[11] Laio F, Porporato A, Ridolfi L, Rodriguez-Iturbe I. Mean first passage times of stochastic processes driven by shot noise. Phys Rev E 2001;63:036105.

[12] Lauenroth WK, Dodd JL, Sims Pl. The effect of water and nitrogen induced stresses on plant community structure in semiarid grassland. Oecologia 1978;36:211–22.

[13] Lauenroth WK, Sala OE, Coffin DP, Kirchner TB. The importance of soil–water recruitment of *Bouteloua gracilis* in the shortgrass steppe. Ecol Appl 1994;4(4):741–9.

[14] Kramer PJ, Boyer JS. Water relations of plants and soils. San Diego: Academic Press; 1995.

[15] Major JA. Climatic index to vascular plant activity. Ecology 1963;44(3):485–98.

[16] Naveh Z. Mediterranean ecosystems and vegetation types in California and Israel. Ecology 1967;48(3):445–4459.

[17] Ng E, Miller PC. Soil moisture relations in the Southern California Caparral. Ecology 1980;61(1):98–107.

[18] Noy-Meir I. Desert ecosystems: environment and producers. Ann Rev Ecol Systemat 1973;4:25–51.

[19] Paruelo JM, Sala OE. Water losses in the Patagonian steppe: a modeling approach. Ecology 1995;76(2):510–20.

[20] Porporato A, Laio F, Ridolfi L, Rodriguez-Iturbe I. Plants in water-controlled ecosystems: active role in hydrologic processes and response to water stress—III. Vegetation water stress. Adv Water Resour 2001;24(7):725–44.

[21] Porporato A, Laio F, Ridolfi L, Caylor K, Rodriguez-Iturbe I. Soil moisture dynamics and water stress along the Kalahari precipitation gradient. J Geophys Res D (Atmospheres), submitted for publication.

[22] Ridolfi L, D'Odorico P, Porporato A, Rodriguez-Iturbe I. Duration and frequency of water stress in vegetation: an analytical model. Water Resour Res 2000;36(8):2297–307.

[23] Ridolfi L, D'Odorico P, Porporato A, Rodriguez-Iturbe I. Impact of climate variability on the vegetation water stress. J Geophys Res (Atmospheres) 2000;105(D14):18013–25.

[24] Robock A, Vinnikov KY, Srinivasan G, Entin JK, Hollinger SE, Speranskaya NA, et al. The global soil moisture data bank. Bull Am Meteor Soc 2001;81(6):1281–99.

[25] Rodriguez-Iturbe I, Entekhabi D, Bras RL. Non-linear dynamics of soil moisture at climate scales, 1, Stochastic analysis. Water Resour Res 1991;27:1899–906.

[26] Rodriguez-Iturbe I, D'Odorico P, Porporato A, Ridolfi L. On the spatial and temporal links between vegetation, climate and soil moisture. Water Resour Res 1999;35(12):3709.

[27] Rodrìguez-Iturbe I, D'Odorico P, Porporato A, Ridolfi L. Tree–grass coexistence in savannas: the role of spatial dynamics and climate fluctuations. Geophys Res Lett 1999;26(2):247–50.
[28] Rodriguez-Iturbe I, D'Odorico P, Porporato A, Ridolfi L. On the spatial and temporal links between vegetation, climate and soil moisture. Water Resour Res 1999c;35(12):3709.
[29] Rodriguez-Iturbe I, Porporato A, Laio F, Ridolfi L. Plants in water-controlled ecosystems: active role in hydrologic processes and response to water stress—I. Scope and general outline. Adv Water Resour 2001;24(7):695–705.
[30] Rodriguez-Iturbe I, Porporato A, Laio F, Ridolfi L. Intensive and extensive use of soil moisture: plant strategies to cope with stochastic water availability. Geophys Res Lett 2001;28(23):4495–7.
[31] Sala OE, Lauenroth WK. Small rainfall events: an ecological role in semiarid regions. Oecologia 1982;53:301–4.
[32] Sala OE, Lauenroth WK, Parton WJ. Long-term soil water dynamics in the short-grass steppe. Ecology 1992;73(4):1175–81.
[33] Sarmiento G. The ecology of the neotropical savannas. Translated by Solbrig O. Cambridge, Mass: Harvard University Press; 1984.
[34] Scholes RJ, Archer SR. Ann Rev Ecol Systemat 1997;28:517–44.
[35] Scholes RJ, Walker BH. An African savanna. Cambridge: Cambridge University Press; 1993.
[36] Singh JS, Milchunas DG, Lauenroth WK. Soil water dynamics and vegetation patterns in a semiarid grassland. Plant Ecol 1998;134(1):77–89.
[37] Waring RH, Running SW. Forest ecosystems. Chennai: Academic Press; 1998.
[38] Cordoba JR, Bras R. Physically based probabilistic models of infiltration, soil moisture, and actual evapotranspiration. Water Resour Res 1983;17(1):93–106.
[39] Salvucci GD. Estimating the moisture dependence of root zone water loss using conditionally averaged precipitation. Water Resour Res 2001;37(5):1357–65.